Proceedings of the ASME 2015 International Manufacturing Science and Engineering Conference
MSEC2015
June 8-12, 2015, Charlotte, North Carolina, USA

MSEC2015-9498

ENERGY EFFICIENCY AND PERFORMANCE OPTIMIZED CONTROL OF A HYBRID FEED DRIVE

Molong Duan, Chinedum E. Okwudire[1]
Mechatronics and Sustainability Research Laboratory
Department of Mechanical Engineering
University of Michigan, Ann Arbor, MI, USA
[1]Contact Author

KEYWORDS
Energy efficiency, precision control, machining, linear motor

ABSTRACT
Linear motor drives (LMDs) are well known to provide significant advantages in terms of positioning speed and precision over traditional screw drives (SDs), making them better suited for high-speed, high-precision machine tools. However, their use in such machine tools is limited by their tendency to consume a lot of electrical energy and cause thermal issues that help drive up costs. A hybrid feed drive (HFD) has been proposed as a possible solution to this dilemma. The HFD combines LMD and SD actuation to achieve speeds and accuracies similar to LMDs while consuming much less energy. This paper explores control strategies to further improve the performance of the HFD without unduly sacrificing its efficiency. First, it highlights two performance limitations of the controller proposed for the HFD in prior work, namely, imperfect tracking and suboptimal feedback gains. Then it compares two approaches for achieving perfect tracking with regard to performance and energy efficiency. Finally, it presents an approach for optimizing the feedback gains of the HFD to achieve the best positioning performance. Simulations and experiments are used to demonstrate significant gains in precise positioning using the methods proposed in this paper, while maintaining superb energy efficiency relative to an equivalent LMD.

1. INTRODUCTION
Feed drives are used for coordinated motion delivery in manufacturing machines. Consequently, their positioning accuracy and speed play a critical role in the quality and productivity of a variety of manufacturing processes, including machining [1]. Most machine tools utilize screw drives (SDs) for actuating their feed axes. The reason is that SDs are cost effective and have high mechanical advantage which allows them to support high cutting forces with very low energy consumption [2–4]. The speed and accuracy of SDs are however limited because of mechanical issues like vibration, wear, backlash and geometric errors of the screw and associated mechanical components [1,5]. To mitigate these shortcomings, linear motor drives (LMDs) are increasingly being resorted to [2,5–7]. LMDs can achieve higher speeds and accelerations than SDs. Moreover, they are not subject to the inaccuracies caused by geometric errors, wear and structural deformations arising from the screw and other mechanical components like bearings, couplers and nuts that are connected to it [1,5]. LMDs are therefore generally more precise than SDs. However, because they have no mechanical advantage, they consume a lot more electrical energy to support cutting forces than SDs. The resultant heat generated has to be removed by cooling systems to prevent thermal issues, thus driving up the cost and energy consumption of the machine [5]. To reduce the energy/heat issues related to linear motors, Okwudire and Rodgers [8] have recently proposed a hybrid feed drive (HFD). Much like hybrid electric vehicles, their proposed HFD synergistically combines a LMD and SD to achieve speeds and accuracies similar to LMDs while consuming much less energy [8,9].

The use of one or more redundant actuators in machine tool feed drives is not new (see for example Refs. [10–14]). When redundant actuators are employed, control effort is often focused on improving the positioning performance of the machine tool [10–13]. The HFD however provides the opportunity to not only improve positioning performance but also energy efficiency through control of the redundant actuators [14]. This paper explores some techniques for controlling the HFD to achieve improved performance at minimal energy costs by exploiting its redundant actuation. The rest of the paper is organized as follows. Section 2 gives a brief overview of the HFD and highlights two weaknesses in the controller proposed for it in prior work – namely imperfect tracking and suboptimal feedback gains. Section 3, investigates two approaches for achieving perfect tracking with regard to performance and energy

efficiency, and then presents an approach for optimizing the feedback gains of the HFD. Simulations and experiments are conducted in Section 4 to demonstrate the benefits of the control techniques presented in this paper for improving the performance and efficiency of the HFD relative to an equivalent LMD, followed by discussions, conclusions and future work.

2. THE HFD AND ITS CONTROLLER

2.1. OVERVIEW OF HFD CONCEPT

Machining operations typically consist of a combination of two modes – rapid traverse (i.e., high-speed, zero-cutting-force positioning moves) and cutting, usually involving low feed rates and large cutting forces. The idea behind the HFD is to: (i) drive the machine table using the LMD during rapid traverse to achieve very high speeds and accelerations with low energy consumption; (ii) drive the table using a low-lead SD during cutting to achieve the required cutting speeds with low energy consumption; (iii) use the LMD to compensate for vibrations and errors introduced by the SD during cutting; and (iv) ensure that the switch between the LMD and SD can be achieved rapidly and energy efficiently at any position of the table within its travel.

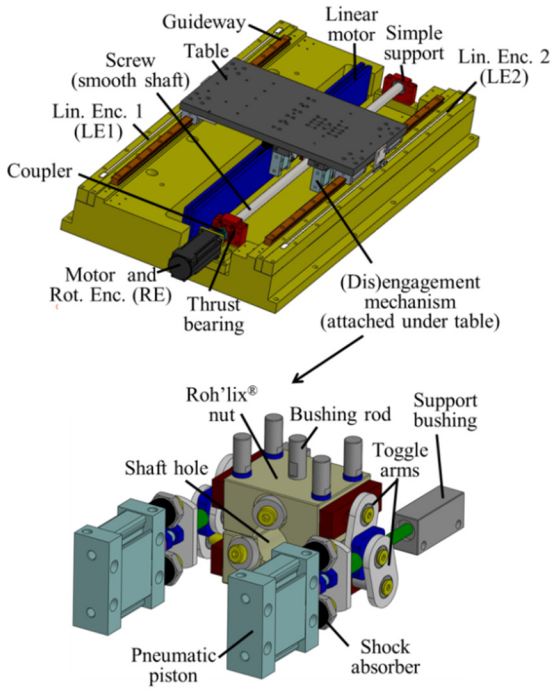

Figure 1: (a) HFD Prototype Proposed by Okwudire and Rodgers [8]

Figure 1 shows the CAD model of a HFD prototype whose design is detailed in [8]. An air core linear motor is employed to drive the table because it does not need to support large cutting forces for which iron core motors are better suited, hence cogging forces are minimized. The SD is driven by a brushless DC motor. To facilitate easy engagement and disengagement of the SD from the table, a traction drive SD which uses a rolling helix (or Roh'lix®) nut [15,16] is employed. The Roh'lix® nut converts rotary motion to linear motion using rolling element ball bearings that trace a screw motion (of lead = 5 mm) along a smooth shaft of 25 mm diameter and 965 mm length. It is designed to carry up to 444 N of thrust force without slippage between the nut and shaft. The Roh'lix® nut comes in two spring-loaded halves that can be separated to disengage the smooth shaft from the nut at any given location. A simple toggle mechanism is designed to separate the two halves of the nut using a pair of fast-acting pneumatic pistons. Note that using a toggle mechanism ensures that no energy is required to keep the nut halves separated.

2.2. ANALYSIS OF HFD'S CONTROLLER

Figure 2(a) shows a slightly simplified version of the controller proposed for the cutting mode of the HFD, when the LMD and SD are coupled together [8]. x_r is the reference position while x_1 and x_2 represent the (equivalent) linear displacements of the rotary and linear motors, respectively. u_1 and u_2 are the corresponding (equivalent) control forces applied to each actuator. The conversion factor, $r_g = lead/(2\pi)$ denotes the gear ratio of the SD. A P-PI feedback (FB) controller, with velocity loop closed using dx_1/dt and position loop closed using x_2, is combined with velocity and acceleration feed forward (FF) loops to control the SD [17]. K_{pp} and K_{vp} are the proportional (P) gains for the position and velocity FB loops, respectively, while K_{vi} is the velocity FB loop's integral (I) gain. K_{vff} and K_{aff} are the velocity and acceleration FF gains. Additionally, the controller has a PD feedback controller with gains K_p and K_d for controlling the LMD to provide position error compensation and active vibration damping.

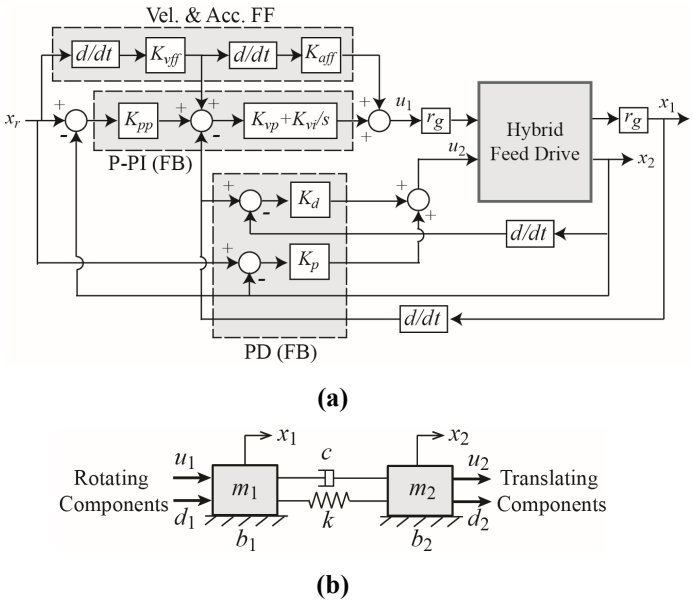

Figure 2: (a) Controller for Cutting Mode of HFD Proposed in Ref. [8], and (b) Two-Mass Model of HFD

A two-mass model like the one shown in Figure 2(b) for the HFD is typically used to model SDs because it is simple and it

captures the first axial/torsional vibration mode of SDs, which is well known to be the bottleneck for controller design [18–21]. m_1 and m_2 are the (equivalent) masses of the rotating and translating components of the HFD, while k and c represent the stiffness and viscous damping coefficients of the connecting mechanical components. b_1 and b_2 are coefficients representing the viscous damping at m_1 and m_2, respectively. x_1, x_2, u_1 and u_2 are the same as in Figure 2(a), while d_1 and d_2 are external disturbance forces (e.g., friction and cutting forces) applied to m_1 and m_2. The equation of motion of the HFD is therefore given by

$$\begin{aligned} m_1\ddot{x}_1 + b_1\dot{x}_1 + c(\dot{x}_1 - \dot{x}_2) + k(x_1 - x_2) &= u_1 + d_1 \\ m_2\ddot{x}_2 + b_2\dot{x}_2 + c(\dot{x}_2 - \dot{x}_1) + k(x_2 - x_1) &= u_2 + d_2 \end{aligned} \tag{1}$$

such that the transfer function of the HFD between its inputs $\mathbf{u} = \{u_1 \quad u_2\}^T$ and $\mathbf{d} = \{d_1 \quad d_2\}^T$ and its output $\mathbf{x} = \{x_1 \quad x_2\}^T$ can be written as

$$\mathbf{x}(s) = \underbrace{\begin{bmatrix} G_{11}(s) & G_{12}(s) \\ G_{21}(s) & G_{22}(s) \end{bmatrix}}_{\mathbf{G}(s)} \left(\mathbf{u}(s) + \mathbf{d}(s)\right) \tag{2}$$

where

$$\begin{aligned} &G_{11} = \frac{m_2 s^2 + (c + b_2)s + k}{den}; \quad G_{22} = \frac{m_1 s^2 + (c + b_1)s + k}{den}; \\ &G_{12} = G_{21} = \frac{cs + k}{den}; \quad den = m_1 m_2 s^4 + a_1 s^3 + a_2 s^2 + a_3 s; \\ &a_1 = b_1 m_2 + b_2 m_1 + c(m_1 + m_2); \\ &a_2 = c(b_1 + b_2) + k(m_1 + m_2) + b_1 b_2; \quad a_3 = (b_1 + b_2)k \end{aligned} \tag{3}$$

The ideal FF controller should be designed to achieve so-called "perfect tracking." This means that it achieves zero tracking error if there is no mismatch between the plant model and the actual plant [22]. In general, when velocity and acceleration FF are applied to a stage modeled as one rigid mass $m = m_1 + m_2$ with no damping, perfect tracking is achieved by setting $K_{vff} = 1$ and $K_{aff} = m$ [17]. When damping exists, an additional FF loop with contribution equal to $(b_1 + b_2)dx_r/dt$ can be added to u_2 in Figure 2(a) so that perfect tracking is achieved. With perfect-tracking FF control in place, all the FB controller needs to do is to correct any deviations from the desired command that may occur due to disturbances or modeling errors of the plant. However, when applied to the two-mass HFD, the basic velocity and acceleration FF control of Figure 2(a) does not yield perfect tracking, as will be demonstrated in Section 4. Furthermore, in Ref. [8], the P-PI and PD gains of the HFD's FB controller were tuned by trial and error, without any guarantee that they were optimal. The next section addresses these two weaknesses in a way that improves the positioning performance and energy efficiency of the HFD relative to an equivalent LMD.

3. OPTIMIZED CONTROLLER FOR HFD

3.1. FEED FORWARD CONTROL

A straightforward way of achieving perfect tracking is to design a FF controller that inverts the plant model. Plant inversion works well if the plant has no non-minimum phase zeros (i.e., "unstable" zeros), which become unstable poles when the plant is inverted [22]. The zeros of HFD's plant **G** given in Eq.(2) are "stable." Therefore, a FF controller that achieves perfect tracking is given by

$$\mathbf{u} = \mathbf{G}^{-1}\begin{Bmatrix} x_{r1} & x_{r2} \end{Bmatrix}^T = \begin{Bmatrix} m_1 s^2 + b_1 s \\ m_2 s^2 + b_2 s \end{Bmatrix} x_r \tag{4}$$

x_{r1} and x_{r2} denote the reference position commands for the SD and LMD, respectively. We have assumed that $x_{r1} = x_{r2} = x_r$, i.e., that the same reference command is sent to both actuators. The implication of the FF control law given in Eq.(4) is that each actuator is responsible for moving the mass to which it is attached, such that the two-mass system moves as a rigid body. Hence we call it rigid-body FF (or RBFF). RBFF contains only s and s^2 terms, so it achieves perfect tracking without involving higher order derivatives of x_r beyond acceleration, making it very attractive especially when x_r is not sufficiently smooth. However, if x_r is smooth enough, it is possible to achieve perfect tracking using the SD only [19–21]; we call this approach screw-drive-based FF (or SDFF). SDFF is achieved by realizing that the motor position x_{r1} need not follow x_r. This is because it is the accurate positioning of the table (i.e., $x_2 = x_{r2} = x_r$) that is of concern in machine tool feed drives. Therefore, x_{r1} can be viewed as an extra degree-of-freedom usable to achieve perfect tracking as follows [21]

$$\begin{aligned} &\begin{Bmatrix} x_{r1} \\ x_r \end{Bmatrix} = \begin{bmatrix} G_{11} & G_{12} \\ G_{21} & G_{22} \end{bmatrix} \begin{Bmatrix} u_1 \\ 0 \end{Bmatrix} \\ &\Rightarrow u_1 = G_{21}^{-1} x_r; \quad x_{r1} = G_{11}u_1 = G_{11}G_{21}^{-1}x_r \end{aligned} \tag{5}$$

Expanding u_1 and x_{r1} in Eq.(5) we get

$$u_1 = \frac{m_1 m_2 s^4 + a_1 s^3 + a_2 s^2 + a_3 s}{cs + k} x_r \tag{6}$$

and

$$x_{r1} = \frac{m_2 s^2 + (c + b_2)s + k}{cs + k} x_r \tag{7}$$

a_1, a_2 and a_3 have been defined in Eq.(3). Notice that u_1 for SDFF contains s^3 and s^4 terms, thus requiring the calculation of the jerk and snap (i.e., the third and fourth time derivatives) of x_r. Therefore, x_r has to be sufficiently smooth for SDFF to be effective. Given a choice between RBFF and SDFF, both of which can achieve perfect tracking, it is of interest to determine which is more efficient. A common measure of the efficiency of

an electric actuator is its resistive power losses (a.k.a. copper losses) given by the equation [23,24]

$$P = \left(\frac{u}{K_m} \right)^2 \tag{8}$$

P is the power lost to heat in the coils of the actuator, u is the (equivalent) force applied by the actuator and K_m represents the motor constant [24] in N/√W. Given the same RMS actuator force, the motor constant provides a measure of the comparative efficiency of each actuator; the larger the constant, the more efficient the motor. Note that the motor constant for rotary motors is provided in Nm/√W. It is converted to N/√W by multiplying it by the factor $1/r_g$, where r_g in m/rad is the gear ratio of the screw given in Section 2.2. In general, the efficiency of a rotary motor is higher than an equivalent linear motor [2]. This is especially true in feed drives like the HFD which use a low-lead SD for which r_g is very small. If K_{m1} and K_{m2} are used to denote the K_m of the rotary and linear motors, respectively, we can say that $K_{m1} > K_{m2}$. Applying Eq.(8) to the FF control forces derived in Eqs. (4) and (6), respectively, for RBFF and SDFF, we get their relative efficiency as

$$\frac{\int P_{SDFF}\,dt}{\int P_{RBFF}\,dt} = \frac{\frac{1}{K_{m1}^2}\int \left(\frac{m_1 m_2}{k} \dddot{x}_r + (m_1 + m_2)\ddot{x}_r \right)^2 dt}{\int \left(\frac{m_1^2}{K_{m1}^2} + \frac{m_2^2}{K_{m2}^2} \right) \ddot{x}_r^2\,dt} \tag{9}$$

where the expressions in the numerator and denominator pertain to the heat generated by SDFF and RBFF, respectively. For the sake of simplicity, the damping terms (i.e., b_1, b_2 and c) have been neglected in deriving Eq.(9). It is reasonable to ignore the integral of snap relative to that of acceleration (for a snap-limited reference trajectory) because snap occurs over very short time intervals. Therefore, the condition for SDFF to be more efficient than RBFF simplifies to

$$\frac{K_{m1}^2}{K_{m2}^2} \geq \left(\frac{2m_1}{m_2} + 1 \right) \tag{10}$$

m_1, which represents the equivalent mass of the rotating components, is usually larger than m_2 [18–21]; but we also know that $K^2_{m1}/K^2_{m2} > 1$, meaning that there is some tradeoff involved. Under the simplifying assumptions made in its derivation, Eq.(10) provides an elegant criterion for determining when to use SDFF over RBFF. However, if the damping or snap terms are not negligible, the relative efficiency of the actuators would depend on the time profile of x_r, and so must be evaluated on a case-by-case basis (e.g., using simulations).

3.2. FEEDBACK CONTROL

The FB control action of the HFD can be derived from the block diagram of Figure 2(a) by setting the FF gains (K_{vff} and K_{aff}) and the reference command x_r equal to zero. Accordingly, we get

$$\begin{aligned} u_1 &= -\left(K_{vi} + sK_{vp} \right) x_1 - \left(K_{pp}K_{vp} + \frac{1}{s} K_{pp}K_{vi} \right) x_2 \\ u_2 &= sK_d x_1 - \left(K_p + sK_d \right) x_2 \end{aligned} \tag{11}$$

Equation (11) can be re-written in a more compact form as

$$\mathbf{u} = -\mathbf{K}\mathbf{x};$$

$$\mathbf{K} = \begin{bmatrix} K_{vi} + K_{vp}s & K_{pp}K_{vp} + K_{pp}K_{vi}/s \\ -K_d s & K_p + K_d s \end{bmatrix} \tag{12}$$

K represents a structured gain matrix that can be optimized to improve FB control performance. Systematic approaches for optimizing such a matrix are available in the literature (e.g., [25–28]). They allow a performance-based objective function with stability constraints to be defined, and then employ numerical techniques to optimize **K**. Such systematic approaches are preferable to the traditional gain tuning procedure for P-PI controllers employed in Ref. [8], where the gains of each control loop are tuned sequentially, starting from the inner to the outer loops.

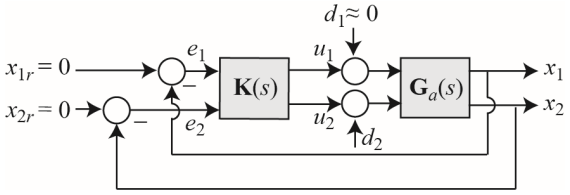

Figure 3: Block Diagram of FB Control of HFD

To optimize **K** systematically, let us represent the HFD's FB controller using the block diagram shown in Figure 3. $\mathbf{G}_a(s)$ is the actual plant dynamics of the HFD, comprising dynamics modeled in $\mathbf{G}(s)$ combined with un-modeled, higher-order dynamics. It is assumed that d_1 (i.e., friction in the rotary motor) is negligible compared to d_2 (i.e., guideway friction and cutting forces). The optimization is performed using a particle swarm technique similar to the one proposed in Refs. [27,28]. The gain matrix is initialized using the **K** tuned by the traditional approach. The objective function is defined as the peak value of the weighted closed-loop frequency response function from input d_2 to output e_2. In other words, it minimizes the influence of guideway friction and cutting forces on the table position error of the controlled system. Lower frequencies are weighted more than higher frequencies in the optimization. Constraints are put in place to ensure that the resulting controller is stable and that it maintains the same margins of stability as those of the traditionally tuned **K**. The result of the optimization is the automatic generation of an optimal gain matrix **K** which significantly improves positioning performance, as is demonstrated in the next section.

4. SIMULATIONS AND EXPERIMENTS

Simulations and experiments are carried out to validate the performance and efficiency of the original and optimized controllers for the HFD relative to an equivalent LMD. Figure 4

shows the HFD prototype used for the simulations and experiments while Table 1 summarizes its performance specifications. It can reach up to 150 m/min speeds at 2.5*g* acceleration when the table is disengaged from the screw, in the rapid traverse mode. It is however designed for a maximum of 10 m/min feed speed at 1*g* acceleration in the cutting mode, when the table is coupled to the screw. The simulations and experiments in this paper are focused on the cutting mode.

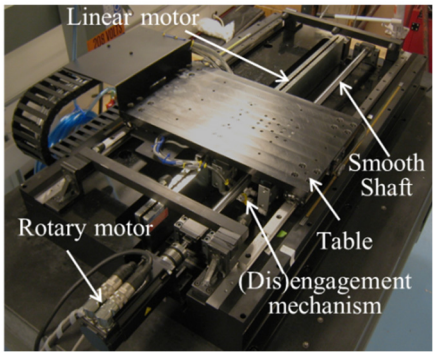

Figure 4: HFD Prototype used for Simulations and Experiments

Travel [mm]	500
Rapid traverse feed rate [m/min]	150
Cutting feed rate [m/min]	10
Rapid traverse acceleration [g]	2.5
Cutting acceleration [g]	1
RMS Feed force [N]	400
Dwell between rapid and cutting modes [ms]	200

Table 1: Performance Specifications of HFD Prototype (Max. Values)

4.1. SIMULATION TESTS AND RESULTS

Simulations are conducted to evaluate the performance and energy efficiency of various FF controllers for the HFD in comparison with FF control for an equivalent LMD (i.e., the linear motor with the SD disengaged). Table 2 summarizes the experimentally identified parameters of the HFD's two-mass model, as well as its motor constants used for simulations.

Table 2: Parameters of HFD Used for Simulations

m_1 [kg]	m_2 [kg]	b_1 [kg/s]	b_2 [kg/s]	c [kg/s]	k [N/μm]	K_{m1} [N/√W]	K_{m2} [N/√W]
639.2	44.3	3456.4	2.3	4686.8	6.8443	380.8	21

Four FF controllers are evaluated:

a) *Traditional FF*: The FF controller shown in Figure 2(a) with $K_{vff} = 1$ and $K_{aff} = m$, applied to the HFD. The additional FF loop discussed in Section 2.2 for damped systems is also incorporated to enhance its performance

b) *RBFF* discussed in Section 3.1, applied to the HFD

c) *SDFF* discussed in Section 3.1, applied to the HFD

d) *LMDFF:* The FF controller for the LMD which is similar to the traditional FF for the HFD with m_1 and b_1 equal to zero [17].

In the simulations, $\mathbf{G}_a(s) = \mathbf{G}(s)$ (i.e., perfect plant model) and $d_1 = d_2 = 0$ are assumed so that no FB controller is needed. This allows the effect of FF control to be evaluated separately from FB. FF control is evaluated by commanding the machine to track two snap-limited reference trajectories x_r over a distance of 100 mm at a speed of 100 mm/s. They are defined as follows

I. *Soft Trajectory:* Acc. limit = 0.1*g*, jerk limit = 6.25 x 10^4 mm/s^3, snap limit = 1.25 x 10^7 mm/s^4

II. *Aggressive Trajectory:* Acc. limit = 1*g*, jerk limit = 4 x 10^6 mm/s^3, snap limit = 8 x 10^9 mm/s^4

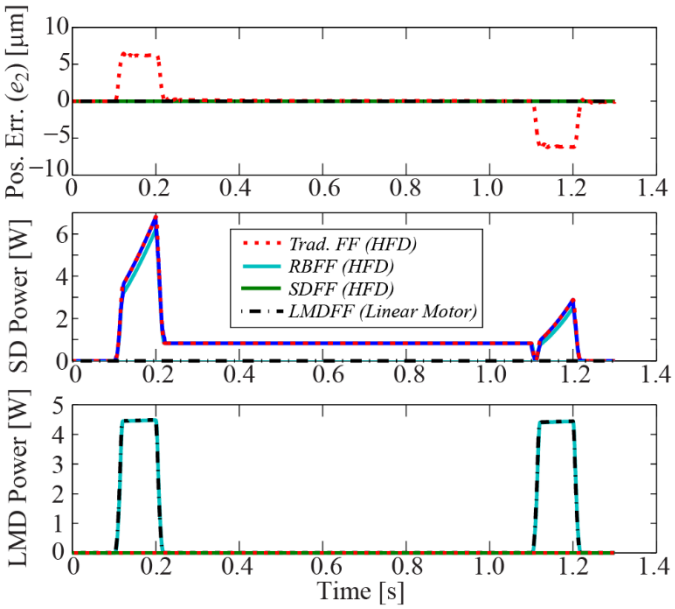

Figure 5: Table Position Error, SD Power and LMD Power of the four FF controllers using the Soft Trajectory

Figure 5 shows the table position error (e_2), the SD and LMD power of the four FF controllers for the soft trajectory, and Figure 6 shows the same results for the aggressive trajectory. Tables 3 and 4 compare the maximum tracking errors and the energy wasted in the form of heat among the controllers for the soft and aggressive trajectories, respectively. As can be seen, the traditional FF is unable to deliver perfect tracking in either case because it cannot compensate for the vibration of the HFD modeled as a two-mass system. RBFF and SDFF are both able to deliver the same perfect tracking achieved by the linear motor (i.e., LMDFF). However, RBFF uses 55% more energy than SDFF for the smooth trajectory, and 31% more energy for the aggressive trajectory. Note that the criterion in Eq.(10) also indicates that SDFF is more efficient than RBFF. The relative efficiency between the two methods is smaller for the aggressive trajectory because of the large additional power the SD requires to compensate for the vibration of the two-mass HFD. LMDFF is the most efficient because the linear motor, acting alone, has much less inertia than the HFD. It therefore makes a lot of sense

for the HFD to use the FF method that produces the same tracking performance as the LMD while having the smallest energy deficit in comparison with the LMD.

Table 3: Max. Position Error, SD Energy, LMD Energy and Total Energy of the Four FF controllers Using the Soft Trajectory

	Trad. FF	*RBFF*	*SDFF*	*LMDFF*
Max. Pos. Err. [μm]	6.44	0	0	0
SD Energy [J]	1.41	1.33	1.40	0
LMD Energy [J]	0	0.84	0	0.84
Total Energy [J]	1.41	2.17	1.40	0.84

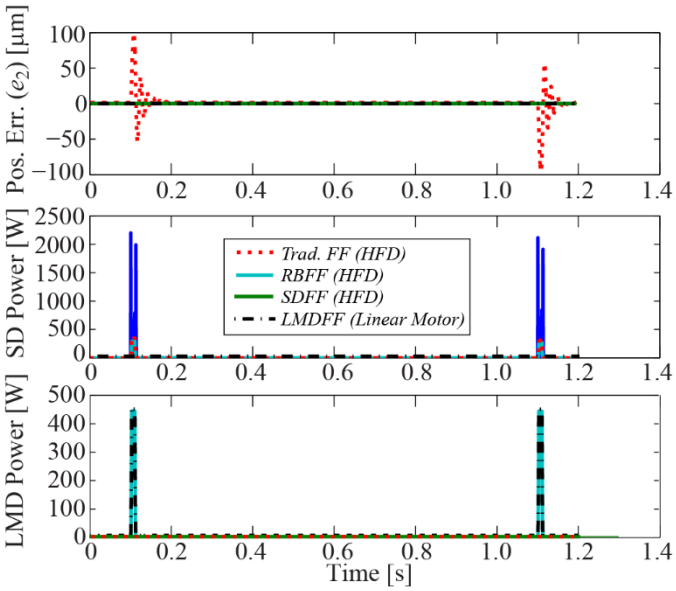

Figure 6: Table Position Error, SD Power and LMD Power of the Four FF Controllers Using the Aggressive Trajectory

Table 4: Max. Position Error, SD Energy, LMD Energy and Total Energy of the Four FF Controllers Using the Aggressive Trajectory

	Trad. FF	*RBFF*	*SDFF*	*LMDFF*
Max. Pos. Err. [μm]	97.8	0	0	0
SD Energy [J]	6.72	5.98	10.70	0
LMD Energy [J]	0	8.14	0	8.14
Total Energy [J]	6.72	14.02	10.70	8.14

4.2. EXPERIMENT RESULTS

Cutting experiments are conducted to evaluate the FB component of the proposed controller with regard to performance and energy efficiency. The following controllers are compared:

a) *Un-optimized P-PI/PD:* Traditionally-tuned P-PI/PD controller for the HFD.

b) *Optimized P-PI/PD:* P-PI/PD controller for the HFD with gain matrix **K** optimized using the approach discussed in Section 3.2

c) *Optimized P-PI:* P-PI controller for the LMD optimized using the approach discussed in Section 3.2.

Table 5: Gains for the three FB Controllers Compared in Experiments

	K_{pp} [1/s]	K_{vp} [A-s/m]	K_{vi} [A/m]	K_p [A/m]	K_d [A-s/m]
Un-opt. P-PI/PD	130	300	60000	50000	600
Opt. P-PI/PD	89	259	1245	199699	427
Opt. P-PI	174	482	84199	N/A	N/A

Table 6: Cutting Parameters for Slotting Operation

Spindle speed	3000 rpm
Tool	3/8” dia. HSS end mill
Number of flutes	4
Feed per tooth	0.025 mm/tooth
Feed rate	300 mm/min
Lubrication	None

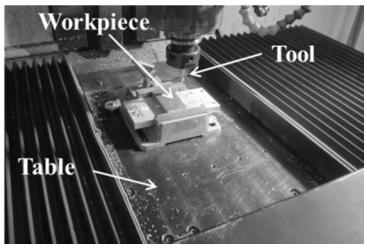

Figure 7: Experimental Setup for Single-axis Slotting Operation using the HFD and LMD

The gains for all three controllers are summarized in Table 5. All controllers have been tuned to have similar stability margins. Notice that the optimized P-PI/PD controller lowers all but one of the gains of the un-optimized P-PI/PD controller, which seems counter-intuitive. Figure 7 shows the set up used for cutting experiments. The HFD prototype of Figure 4 is mounted on the x axis of a FADAL VMC 4020 3-axis milling machine to cut a 50 mm long, 1.5 mm deep slot in an AISI 1018 steel workpiece. Table 6 summarizes the key cutting parameters for the operation. Figure 8 shows a comparison of the table position errors (e_2) measured from the linear encoder, and the SD and LMD energy for each controller considered. Note that the power signals are not plotted (as in Figures 5 and 6) because they are too oscillatory and overlapping to make out the differences among them. Table 7 summarizes the maximum and RMS table position errors, as well as the SD, LMD and total energy for each controller. Notice that the optimized P-PI/PD controller for the HFD is significantly better than the un-optimized controller in terms of positioning performance and energy efficiency. Its maximum and RMS errors are both 56% less, and the energy it wastes in heat is 53% less than the un-optimized P-PI/PD. Its positioning

performance is very comparable to the LMD's but its efficiency is 71% better.

Table 7: Max./RMS Position Error, SD, LMD and Total Energy of the Three FB Controllers during a Single-axis Slotting Operation

	Un-Opt. P-PI/PD	*Opt. P-PI/PD*	*Opt. P-PI*
Max. Pos. Err. [μm]	28.59	11.66	11.47
RMS. Pos. Err. [μm]	12.95	5.65	4.33
SD Energy [J]	89.12	41.76	N/A
LMD Energy [J]	222.92	104.45	509.43
Total Energy [J]	312.03	146.21	509.43

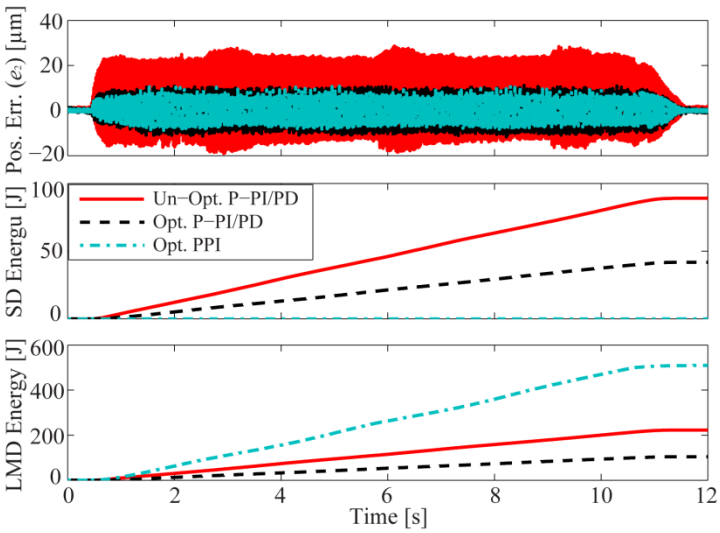

Figure 8: Table Position Error, SD Energy and LMD Energy of the Three FB Controllers during a Single-axis Slotting Operation

5. CONCLUSION AND FUTURE WORK

This paper has presented techniques for improving the positioning precision and energy efficiency of a hybrid feed drive (HFD) relative to an equivalent linear motor drive (LMD). Two weaknesses of the controller originally proposed for the HFD are highlighted, namely, imperfect tracking and sub-optimal feedback gains. Two approaches for achieving perfect tracking are compared with regard to energy efficiency and a simple criterion for selecting the more efficient one is proposed. A systematic approach for optimizing the feedback gains of the HFD's controller is also presented. The HFD, controlled using its original (suboptimal) controller and optimized controllers (proposed in this paper) is compared in simulations and experiments to an equivalent LMD. Remarkable improvements in positioning performance and energy efficiency are demonstrated by the optimized controllers. Future work will investigate how to re-structure the HFD's controllers to further improve performance and efficiency.

6. ACKNOWLEDGEMENTS

This work is funded by the National Science Foundation's CAREER Award #1350202: Dynamically Adaptive Feed Drives for Smart and Sustainable Manufacturing.

REFERENCES

[1] Altintas, Y., Verl, A., Brecher, C., Uriarte, L., and Pritschow, G., 2011, "Machine tool feed drives," CIRP Ann. - Manuf. Technol., **60**(2), pp. 779–796.

[2] Pritschow, G., 1998, "A Comparison of Linear and Conventional Electromechanical Dives," CIRP Ann. - Manuf. Technol., **47**(2), pp. 541–548.

[3] Dahmus, J. B., and Gutowski, T. G., 2004, "An Environmental Analysis of Machining," Manufacturing Engineering and Materials Handling Engineering, ASME, pp. 643–652.

[4] Diaz, N., Helu, M., Jarvis, A., Tönissen, S., Dornfeld, D., and Schlosser, R., 2009, "Strategies for Minimum Energy Operation for Precision Machining," Lab. Manuf. Sustain.

[5] Pritschow, G., and Philipp, W., 1990, "Direct Drives for High-Dynamic Machine Tool Axes," CIRP Ann. - Manuf. Technol., **39**(1), pp. 413–416.

[6] Robert, A., 1997, "Attack of the linear motors," Manuf. Eng.

[7] Sato, K., Katori, M., and Shimokohbe, A., 2013, "Ultrahigh-Acceleration Moving-Permanent-Magnet Linear Synchronous Motor With a Long Working Range," IEEE/ASME Trans. Mechatronics, **18**(1), pp. 307–315.

[8] Okwudire, C., and Rodgers, J., 2013, "Design and control of a novel hybrid feed drive for high performance and energy efficient machining," CIRP Ann. - Manuf. Technol., **62**(1), pp. 391–394.

[9] Kale, S., Dancholvichit, N., and Okwudire, C., 2014, "Comparative LCA of a Linear Motor and Hybrid Feed Drive under High Cutting Loads," Procedia CIRP, **14**, pp. 552–557.

[10] Elfizy, A. T., Bone, G. M., and Elbestawi, M. A., 2005, "Design and control of a dual-stage feed drive," Int. J. Mach. Tools Manuf., **45**(2), pp. 153–165.

[11] Gordon, D. J., and Erkorkmaz, K., 2012, "Precision control of a T-type gantry using sensor/actuator averaging and active vibration damping," Precis. Eng., **36**(2), pp. 299–314.

[12] Fujita, T., Matsubara, A., Kono, D., and Yamaji, I., 2010, "Dynamic characteristics and dual control of a ball screw drive with integrated piezoelectric actuator," Precis. Eng., **34**(1), pp. 34–42.

[13] Frey, S., Groh, K., and Verl, A., 2012, "Semi-active damping of drive systems," J. Vib. Control, **19**(5), pp. 742–754.

[14] Halevi, Y., Carpanzano, E., Montalbano, G., and Koren, Y., 2011, "Minimum energy control of

redundant actuation machine tools," CIRP Ann. - Manuf. Technol., **60**(1), pp. 433–436.
[15] "Roh'Lix® Linear Actuators" [Online]. Available: http://www.zero-max.com/linear-motion-control-c-24-l-en.html. [Accessed: 17-Dec-2014].
[16] Buice, E. S., Otten, D., Yang, R. H., Smith, S. T., Hocken, R. J., and Trumper, D. L., 2009, "Design evaluation of a single-axis precision controlled positioning stage," Precis. Eng., **33**(4), pp. 418–424.
[17] Altintas, Y., and Okwudire, C. E., 2009, "Dynamic stiffness enhancement of direct-driven machine tools using sliding mode control with disturbance recovery," CIRP Ann. - Manuf. Technol., **58**(1), pp. 335–338.
[18] Varanasi, K., and Nayfeh, S., 2004, "The dynamics of lead-screw drives: low-order modeling and experiments," J. Dyn. Syst. Meas. Control, **126**, pp. 388–396.
[19] Kamalzadeh, a., and Erkorkmaz, K., 2007, "Compensation of Axial Vibrations in Ball Screw Drives," CIRP Ann. - Manuf. Technol., **56**(1), pp. 373–378.
[20] Okwudire, C., and Altintas, Y., 2009, "Minimum Tracking Error Control of Flexible Ball Screw Drives Using a Discrete-Time Sliding Mode Controller," J. Dyn. Syst. Meas. Control, **131**(5), p. 051006.
[21] Gordon, D. J., and Erkorkmaz, K., 2013, "Accurate control of ball screw drives using pole-placement vibration damping and a novel trajectory prefilter," Precis. Eng., **37**(2), pp. 308–322.
[22] Tomizuka, M., 1987, "Zero Phase Error Tracking Algorithm for Digital Control," J. Dyn. Syst. Meas. Control, **109**(1), p. 65.
[23] Kollmorgen, 2011, "Kollmorgen Direct Drive Linear Motor Selection Guide KM_CA_00084_RevA_EN," p. 75 [Online]. Available: http://www.kollmorgen.com/zu-za/products/motors/direct-drive/direct-drive-linear/_literature/kollmorgen-direct-drive-linear-motor-selection-guide/. [Accessed: 21-Dec-2014].
[24] Hiemstra, D. B., Parmar, G., and Awtar, S., 2014, "Performance Tradeoffs Posed by Moving Magnet Actuators in Flexure-Based Nanopositioning," IEEE/ASME Trans. Mechatronics, **19**(1), pp. 201–212.
[25] Krohling, R. A., and Rey, J. P., 2001, "Design of optimal disturbance rejection PID controllers using genetic algorithms," IEEE Trans. Evol. Comput., **5**(1), pp. 78–82.
[26] Ho, S.-J., Ho, S.-Y., and Shu, L.-S., 2004, "OSA: orthogonal simulated annealing algorithm and its application to designing mixed H2/H∞ optimal controllers," IEEE Trans. Syst. Man, Cybern. - Part A Syst. Humans, **34**(5), pp. 588–600.
[27] Maruta, I., Kim, T.-H., and Sugie, T., 2009, "Fixed-structure controller synthesis: A meta-heuristic approach using simple constrained particle swarm optimization," Automatica, **45**(2), pp. 553–559.
[28] Zamani, M., Sadati, N., and Ghartemani, M. K., 2009, "Design of an H∞ PID controller using particle swarm optimization," Int. J. Control. Autom. Syst., **7**(2), pp. 273–280.